

Determination of exchange constants of Heusler compounds by Brillouin light scattering spectroscopy: application to Co_2MnSi

J. Hamrle*, O. Gaier, Seong-Gi Min, B. Hillebrands

Fachbereich Physik and Forschungszentrum OPTIMAS,

Technische Universität Kaiserslautern,

Erwin-Schrödinger-Straße 56, D-67663 Kaiserslautern, Germany

Y. Sakuraba

Magnetic Materials Laboratory, Institute for Materials Research (IMR),

Tohoku University, Katahira 2-1-1, Sendai 980-8577, Japan

Y. Ando

Department of Applied Physics, Graduate School of Engineering,

Tohoku University, Aoba-yama, Sendai 980-8579, Japan

Abstract

Brillouin light scattering spectroscopy from so-called standing spin waves in thin magnetic films is often used to determine the magnetic exchange constant. The data analysis of the experimentally determined spin-wave modes requires an unambiguous assignment to the correct spin wave mode orders. Often additional investigations are needed to guarantee correct assignment. This is particularly important in the case of Heusler compounds where values of the exchange constant vary substantially between different compounds. As a showcase, we report on the determination of the exchange constant (exchange stiffness constant) in Co_2MnSi , which is found to be $A = 2.35 \pm 0.1 \mu\text{erg}/\text{cm}$ ($D = 575 \pm 20 \text{ meV } \text{Å}^2$), a value comparable to the value of the exchange constant of Co.

PACS numbers: 75.30.Et, 78.35.+c, 75.30.Ds, 75.50.Cc

* Corresponding author: J. Hamrle, email: hamrle@physik.uni-kl.de

I. INTRODUCTION

The investigation of electron-electron interactions in half-metallic ferromagnetic Heusler compounds is an important issue in order to understand the strong temperature dependence of spin polarization of these materials. One of the key parameters in this context is the magnetic exchange constant (in the following simply referred to as exchange constant) which describes the strength of the exchange interaction between two spins inside a ferromagnetic system. Brillouin light scattering (BLS) spectroscopy from standing spin-waves in thin magnetic films is a well-established technique for the study of exchange interaction in various material systems [1, 2, 3]. However, the application of this experimental technique for the determination of exchange constants in thin films of Heusler compounds presents some difficulties, which, as will be discussed in this article, are mostly related to an ambiguity in the assignment of the measured mode frequencies to the correct standing spin-wave mode orders. The goal of this article is to show in detail how the values of exchange constants are determined from the BLS spectra measured on thin films of Heusler compounds as well as to discuss the difficulties in the extraction of the exchange constants from the experimental data. For this purpose, we present BLS studies of Co_2MnSi films in this article.

In the following, we briefly describe the investigated Co_2MnSi films and the determination of the exchange constant by means of BLS. Thereafter, the experimental results of BLS studies performed on Co_2MnSi thin films are presented, and a procedure leading to the correct mode assignment is discussed.

II. EXPERIMENTAL DETAILS

The investigated Co_2MnSi films with thicknesses $t = 20, 30, 40, 60$ and 80 nm were epitaxially grown on a $\text{MgO}(100)$ substrate covered by a 40 nm thick $\text{Cr}(100)$ buffer layer. For the deposition of the Co_2MnSi layers, inductively coupled plasma-assisted magnetron sputtering was employed. A post-growth annealing at 500°C provided Co_2MnSi films with a predominant $L2_1$ order, which was confirmed by x-ray diffraction (XRD) measurements. The films were covered by a 1.3 nm thick Al protective layer to prevent sample oxidation.

The BLS measurements presented in this article were performed at room temperature in the magneto-static surface mode geometry where the magnetic field \vec{H} is applied in the

plane of the sample and perpendicular to the plane of light incidence i.e. perpendicular to the transferred wave vector q_{\parallel} of the detected magnons. A diode pumped, frequency doubled Nd:YVO₄ laser with a wavelength of $\lambda = 532$ nm was used as a light source. A detailed description of the BLS setup used in this work can be found for example in Refs. [4, 5]. The BLS spectra of Co₂MnSi films with varying thickness t were recorded both at different values of the external magnetic field \vec{H} and at different angles of incidence of the probing light beam φ , i.e., the angle between the direction of the incident laser beam and the film normal. The former is necessary to confirm the magnonic origin of peaks, whereas the latter allows for the detection of spin waves with different transferred wave vectors q_{\parallel} ($q_{\parallel} = 4\pi/\lambda \sin \varphi$). As will be shown later on in this article, q_{\parallel} dependent measurements of BLS spectra are required for an unambiguous separation of the dipole dominated magnetostatic surface wave, also called Damon-Eshbach mode (DE), from the exchange dominated perpendicular standing spin waves (PSSW).

The analytical expression of frequencies of DE and PSSW modes is presented e.g. in Refs. [6, 7, 8]. DE mode is characterized by an exponential decay of the amplitude of the dynamic magnetization [20] over the film thickness t and their nonreciprocal behavior (i.e., reversal of the spinwave propagation direction causes that maximal amplitude of the dynamic magnetization reverse to the opposite interface of the FM film). The amplitude of the dynamic magnetization of a PSSW mode over the film thickness z is proportional to $\cos(m\pi z/t)$, where the positive integer m denotes the quantization number of the standing spin wave.

To determine the values of the exchange constant of Co₂MnSi, all three dependencies of the experimental spin-wave frequencies (\vec{H} , t , q_{\parallel}) are compared with simulations which were performed using a theoretical model described in detail in Ref. [9]. The exchange constant A , the Landau g -factor, the saturation magnetization M_S and the magnetic anisotropies are the free parameters in these simulations. Because our previous BLS investigations of Co₂MnSi films have shown very small anisotropy in L2₁ ordered Co₂MnSi films [6], the anisotropy values were set to zero.

As follow from the analytical expressions [6, 7, 8], for small spinwave wavevector used in our investigations, the frequency of the DE mode depends only marginally on the value of A , i.e., DE mode frequency is particularly determined by the values of M_S and g . On the other hand, the frequencies of the PSSW modes are particularly determined by the A/M_S

ratio and g . Furthermore, the g -factor is easy to determine independently, as it scales with the slope of the BLS frequency on applied magnetic field, df/dH . Therefore, the fitting procedure is not underdetermined and the parameters M_S , A/M_S and g are found rather independently each other, providing a high reliability (low correlation) of the fitted values.

III. RESULTS AND DISCUSSION

Examples of BLS spectra collected from 20, 40, 60 and 80 nm thick Co_2MnSi films are shown in Fig. 1(a). The spectra were recorded at an external magnetic field of $H = 1.5$ kOe and a transferred wave vector of $q_{\parallel} = 1.67 \cdot 10^5 \text{ cm}^{-1}$ (i.e. $\varphi = 45^\circ$). The magnetic origin of the peaks presented in Fig. 1(a) is confirmed by H -dependent measurements, demonstrated in Fig. 1(b) for the case of the 40 nm thick Co_2MnSi film. The peak positions in both the Stokes (negative frequencies) and the anti-Stokes (positive frequencies) part of the spectrum move towards higher frequencies upon increasing the field, revealing their magnetic origin. Figure 1(c) shows the BLS spectra recorded for the 80 nm thick Co_2MnSi film for different spin-wave wavevectors q_{\parallel} . Compared to the PSSW modes, the DE mode exhibits a much stronger dependence on the wavevector. Therefore, the peaks originating from the DE mode excitation can be easily identified, whereas the spectral positions of the PSSW modes remain nearly unchanged (Fig. 1(c)). As expected, the frequency of the DE mode increases with increasing film thickness whereas the frequencies of the PSSW modes shift to lower values (Fig. 1(a)).

Results of numerical simulations (solid lines) are shown in Fig. 2 along with the experimentally determined BLS frequencies (\blacktriangle , \blacktriangledown represent Stokes, anti-Stokes frequencies, respectively) for two different values of the exchange constant A . The saturation magnetization $M_S = 970 \text{ emu/cm}^3$ (corresponding to $\mu = 4.72 \mu_B/\text{f.u.}$) and Landau g -factor $g = 2.05$ is found for both values of A and is in agreement with previous investigations (e.g. [10, 11, 12]). An equally good agreement between the simulations and the experimental data points is achieved for $A = 2.35 \pm 0.1 \mu\text{erg/cm}$ ($D = 575 \pm 20 \text{ meV \AA}^2$) (Fig. 2(a-c)) and $A = 0.60 \pm 0.05 \mu\text{erg/cm}$ ($D = 145 \pm 10 \text{ meV \AA}^2$) (Fig. 2(d-f)), respectively. When $A = 2.35 \pm 0.1 \mu\text{erg/cm}$, the calculations describe all observed PSSW modes. The A value, however, is surprisingly large, being nearly as large as the exchange constant reported for Co(fcc) ($A = 2.73 \mu\text{erg/cm}$, $D = 466 \text{ meV \AA}^2$) or Co(hcp) ($A = 2.85 \mu\text{erg/cm}$,

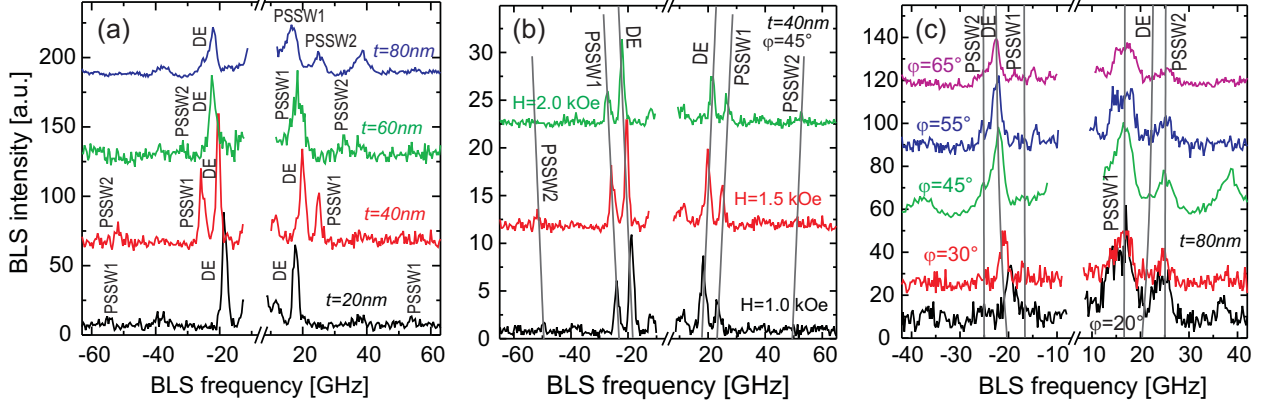


FIG. 1: (Color online) BLS spectra of (a) Co_2MnSi films with different thicknesses t acquired at an applied external field $H = 1.5$ kOe and a transferred wave vector $q_{\parallel} = 1.67 \cdot 10^5 \text{ cm}^{-1}$, (b) 40 nm thick Co_2MnSi film recorded at different values of H at $q_{\parallel} = 1.67 \cdot 10^5 \text{ cm}^{-1}$, and (c) 80 nm thick Co_2MnSi film measured at $H = 1.5$ kOe and different angles of incidence φ , i.e., different transferred wave vectors q_{\parallel} . The full line is a guide to the eye, showing expected peak positions as follow from the model.

$D = 435 \text{ meV \AA}^2$) [2]. In the second case where $A = 0.6 \mu\text{erg/cm}$, only even PSSW modes seem to be observed in the experiment.

Obviously from the fit alone, the correct value of the exchange constant can not be obtained due to the ambiguity in mode order assignment. To find out which value of the exchange constant is the correct one, we have performed analytical calculations of the BLS intensities. In particular, we have examined under which conditions the BLS intensity becomes zero for odd PSSW modes only. The used analytical approach (presented in Appendix A) combines an expression for the BLS intensity, as proposed by Buchmeier *et. al.* [3, 13], and the analytical expression of the depth selectivity of the MOKE effect by Hamrle *et. al.* [14]. The calculations indicate that when conditions (A8) and (A9) derived in the Appendix A are fulfilled, the BLS intensity will be zero for all odd modes. Using the complex refractive index of Co_2MnSi $N^{(CMS)} = 1.1 + 1.1i$ [15], an incidence angle φ of 45° and a thickness t of 20 nm, the value of conditions (A8) and (A9) becomes $4\Re(N_z)t/\lambda = 0.15$ and $4\Im(N_z)t/\lambda = 0.18$, respectively. Those values are far from an odd integer and integer, respectively, as required by conditions (A8) and (A9). This proves that all BLS modes in our Co_2MnSi films should contribute with significant scattering cross section. Hence the exchange constant of Co_2MnSi

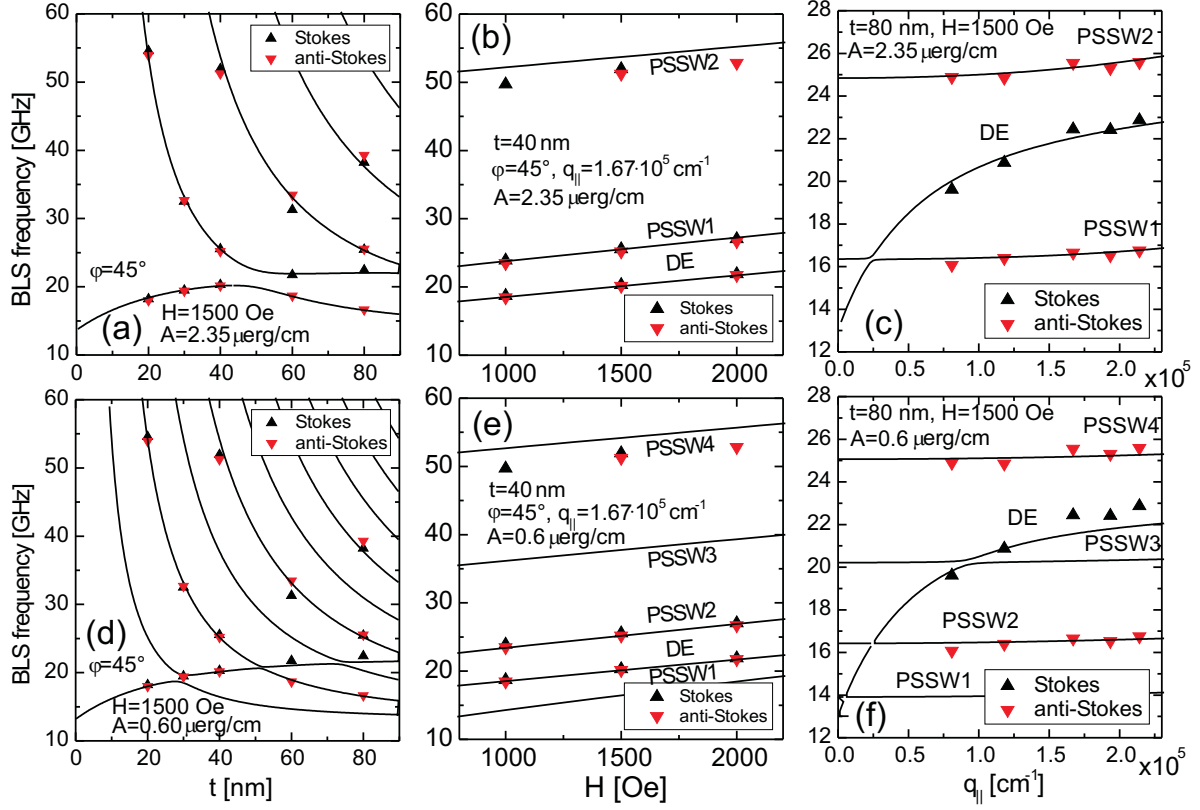


FIG. 2: (Color online) Comparison of calculated (solid lines) and experimental (symbols) BLS frequencies as a function of (a,d) the Co_2MnSi thickness t , (b,e) the external magnetic field H and (c,f) the transferred spin-wave wavevector q_{\parallel} . Experimental data points correspond to the BLS spectra presented in Fig. 1. Triangles up (down) represent Stokes (anti-Stokes) frequencies. Calculation were performed using the exchange constant (a-c) $A = 2.35 \pm 0.1 \mu\text{erg}/\text{cm}$ and (d-f) $A = 0.6 \pm 0.1 \mu\text{erg}/\text{cm}$. The remaining parameters used in the calculations are the saturation magnetization $M_S = 970 \text{ emu}/\text{cm}^3$ and the Landau g -factor $g = 2.05$. The magnetic anisotropies are neglected.

is $A = 2.35 \pm 0.1 \mu\text{erg}/\text{cm}$ (i.e. exchange stiffness $D = 575 \pm 20 \text{ meV} \text{ \AA}^2$), which was determined from the calculations presented in Fig. 2(a-c), that predicted all experimentally observed modes.

Here, we would like to comment on the values of the exchange constant reported for Co_2MnSi by different groups. In Ref. [16], the value of exchange stiffness was determined to be $D = 466 \text{ meV} \text{ \AA}^2$ (i.e. $A = 1.93 \mu\text{erg}/\text{cm}$), using the temperature dependence of the saturation magnetization. This value is rather close to the one we have determined in

our BLS investigations. In Ref. [10], the value of exchange stiffness was estimated to be $D_B = 1.9 \cdot 10^{-9} \text{Oe cm}^2$ (i.e. $D = 225 \text{ meV \AA}^2$, $A = 0.97 \mu\text{erg/cm}$) from FMR investigations, which is much lower compared with our results. This discrepancy might originate from the fact that in Ref. [10] asymmetrical pinning conditions were assumed (i.e., the dynamic magnetization is pinned at one interface, whereas it is unpinned at the second one). In our samples, this condition does not apply due to the following considerations. As can be seen in Fig. 2, the frequencies of the DE mode exhibit equal values in both the Stokes and the anti-Stokes part of the spectrum. Since the Stokes and anti-Stokes DE modes are bound to opposite interfaces of the FM layer, it shows that in our Co_2MnSi films both interfaces are magnetically equivalent.

Finally, we would like to note that in our previous article reporting on BLS studies of Co_2MnSi films [6] the assumption that only even PSSW modes are observed has been used. In view of the results presented here, the conclusions of this article remain valid. The values of the exchange constant in Fig. 9(b) in Ref. [6], however, must be scaled by a factor 5 to get the correct values.

IV. CONCLUSION

Using the case of Co_2MnSi thin films, we demonstrated in detail how the values of exchange constants are determined from the BLS measurements and carefully discussed different values of A proposed by numerical simulations. The value of Co_2MnSi is found to be $A = 2.35 \pm 0.1 \mu\text{erg/cm}$ ($D = 575 \pm 20 \text{ meV \AA}^2$), in agreement with the value determined from the temperature dependence of the magnetization [16]. The found value of exchange is comparable to the value of exchange constant of Co. The pinning conditions for the dynamic magnetization are found to be equal for both $\text{Cr/Co}_2\text{MnSi}$ and $\text{Al/Co}_2\text{MnSi}$ interfaces.

V. ACKNOWLEDGMENT

The project was financially supported by the Research Unit 559 “*New materials with high spin polarization*” funded by the Deutsche Forschungsgemeinschaft, and by the Stiftung Rheinland-Pfalz für Innovation. We thank M. Buchmeier for stimulating discussions.

APPENDIX A: DEPTH SENSITIVITY OF BRILLOUIN LIGHT SCATTERING

The BLS intensity from a single FM layer of thickness t is given by [13]

$$I^{(\text{BLS})} = I_0 \left| \int_0^t [-L(z)m_L(z) + P(z)m_p(z)] dz \right|^2, \quad (\text{A1})$$

where $m_L(z)$ and $m_P(z)$ are the depth profiles of the dynamic magnetization through the FM layer in longitudinal (i.e. in the plane of the sample and in the plane of light incidence) and polar (i.e. out-of-plane) directions, respectively. $L(z)$, $P(z)$ are complex depth sensitivity functions of the off-diagonal reflectivity coefficient r_{sp} for longitudinal $M_L(z)$ and polar $M_P(z)$ static magnetization profiles [13, 14]

$$r_{sp}(\vec{M}) = r_{sp}(M=0) + \int_0^t [L(z)M_L(z) + P(z)M_P(z)] dz. \quad (\text{A2})$$

The dependence of $L(z)$, $P(z)$ on depth z is the same for both of them. Assuming that the substrate has a refractive index identical to the refractive index of the FM layer, the analytical terms of $L(z)$ and $P(z)$ may be written as [14]

$$L(z) = L(0) \exp[-4\pi i N_z z / \lambda] \quad (\text{A3})$$

$$P(z) = \gamma L(z), \quad (\text{A4})$$

where the complex coefficient γ is the ratio of $P(0)$ and $L(0)$. N_z is the normalized wave vector in polar direction $N_z = \sqrt{(N^{(\text{fm})})^2 - (N^{(\text{air})})^2 \sin^2 \varphi}$, where $N^{(\text{fm})}$ and $N^{(\text{air})}$ are the refractive indices of the FM layer and air, respectively, and φ is the angle of incidence of the probing light beam with respect to the sample's normal. Note that if the refractive index of the substrate is different from the one of the FM layer, the analytical expressions become more complex. However the basic features (i.e. continuous decay of the amplitude and continuous shift of the phase) remain valid.

Using the open (anti-pinning) boundary conditions at the interfaces of the FM layer, the depth profile of the dynamic magnetization of a PSSW mode of the m -th order reads [8]

$$m_L(z, \tau) = m_0 \cos(m\pi z/t) \cos(\omega_{sw}\tau) \quad (\text{A5})$$

$$m_P(z, \tau) = m_0 \varepsilon \cos(m\pi z/t) \cos(\omega_{sw}\tau + \pi/2), \quad (\text{A6})$$

where ω_{sw} and τ are the frequency of the spin-wave mode and time, respectively. The magnetization vector follows an elliptical trajectory, with ellipticity ε . Therefore, the m_L and m_P magnetization components are shifted by $\pi/2$ in their time dependence.

Combining Eqs.(A1, A3 – A6) and integrating over the thickness of the FM layer and averaging over time, we obtain

$$I^{(\text{BLS})} = \frac{1}{2}I_0(1 + |\varepsilon\gamma|^2) \left| \frac{L(0)\alpha t m_0}{m^2\pi^2 - \alpha^2} \right|^2 |1 - \exp(-i\alpha)(-1)^m|^2, \quad (\text{A7})$$

with α being a dimensionless parameter defined as $\alpha = 4\pi N_z t/\lambda$.

The total BLS intensity $I^{(\text{BLS})}$ is zero when the last term in Eq.(A7) is zero. For odd m , the intensity is zero when the following conditions hold

$$4\Re(N_z)t/\lambda = (2k + 1) \quad (\text{A8})$$

$$4\Im(N_z)t/\lambda = l \quad (\text{A9})$$

where k and l are both integers. Note that for $m = 2k + 1$, the denominator in Eq. (A7) becomes zero as well, which would also provide a zero BLS intensity. For even m , $I^{(\text{BLS})}$ is zero when

$$2\Re(N_z)t/\lambda = k \quad (\text{A10})$$

$$4\Im(N_z)t/\lambda = l. \quad (\text{A11})$$

where k and l are again integers, respectively.

APPENDIX B: UNITS OF EXCHANGE

Throughout the literature, the exchange is expressed in at least four different variables, making the direct comparison of exchange values difficult. This situation is further complicated by the use of both cgs and SI units, as well as the lack of a unique nomenclature. Here, we give a short overview of different definitions of exchange and the conversion between them.

The energy of a single magnon (i.e. a spin wave, where one single spin in one period of spin wave is reversed) having wave vector k is given by [17]

$$E = \hbar\omega = Dk^2, \quad (\text{B1})$$

where D is called the exchange stiffness (which is sometimes referred to as the spin-wave stiffness), ω is the angular frequency of the spin wave, and \hbar is the reduced Planck constant. The routinely used units of D are meV \AA^2 for both cgs and SI units.

Alternatively, the exchange is expressed as the strength of the effective field D_B created by the exchange energy of the spin wave. As D , D_B is also often called the exchange stiffness. Neglecting a dipolar contribution to the spin wave (i.e. assuming a large value of k), the angular frequency of a spin wave is given by

$$\frac{\omega}{g\gamma_0} = (B + D_B k^2) \quad (\text{B2})$$

where ω is the angular frequency of the spin wave, g is Landau g -factor, B is an external field and $\gamma_0 = e/(2m_e) = 8.793 \cdot 10^{10} \text{ s}^{-1}\text{T}^{-1}$ is the gyromagnetic ratio and e and m_e are the charge and the rest mass of an electron, respectively. Units of D_B are Oe cm² in cgs, and T m² or J A⁻¹ in SI.

Another description of the exchange is provided by the exchange constant A (sometimes also called the exchange stiffness). Within this description, the energy density $E/V = \mathcal{E}$ of a given continuous magnetization distribution $\vec{m}(\vec{r})$ within space is given by

$$E/V = \mathcal{E} = A|\nabla\vec{m}|^2, \quad (\text{B3})$$

where $\vec{m} = \vec{M}/M_S$ is the reduced magnetization and M_S is the saturation magnetization. Units of A are erg/cm in cgs and J/m in SI. Assuming a reduced magnetization \vec{m} in form of a spin wave with wavevector k , the effective field of such a spin wave is

$$B_{\text{eff}} = -\nabla_M \mathcal{E} = \frac{2A}{M_S} k^2. \quad (\text{B4})$$

Comparing Eqs. (B1–B4), the conversion between D , D_B and A are (valid both in SI and cgs)

$$D_B = 2A/M_S \quad (\text{B5})$$

$$D_B = \frac{D}{g\gamma_0\hbar} \quad (\text{B6})$$

$$A = \frac{DM_S}{2g\gamma_0\hbar} \quad (\text{B7})$$

Note that the conversion between SI and cgs for the exchange constant is given by: 1 erg/cm=10⁻⁵ J/m. For the saturation magnetization 1 emu/cm³=1000 A/m. If $M_S = 1 \text{ emu/cm}^3$, then $4\pi M_S = 4\pi \text{ G}$ (i.e. in unit of Gauss).

Finally, here we mention a description of exchange coming from the effective Heisenberg Hamiltonian with classical spins

$$E = - \sum_{i \neq j} J_{ij} \vec{s}_i \cdot \vec{s}_j, \quad (\text{B8})$$

where J_{ij} is the exchange interaction energy between two spins at positions i, j and s_i, s_j are unit vectors pointing in the direction of local magnetic moments at sites i, j , respectively. Assuming that a unit cell contain a single atom, then the spin-wave energy $E(\vec{k})$ is related to the exchange parameters J_{ij} by a simple Fourier transformation [18]

$$E(\vec{k}) = \frac{4\mu_B}{\mu} \sum_{j \neq 0} J_{0j} \left(1 - \exp(i\vec{k} \cdot \vec{R}_{0j}) \right), \quad (\text{B9})$$

where $\vec{R}_{0j} = \vec{R}_0 - \vec{R}_j$ denotes a lattice vector in real space, \vec{k} is the spinwave vector, μ is the magnetic moment per atom and μ_B is the Bohr magneton. The exchange stiffness D is given by the curvature of the spin-wave dispersion $E(\vec{k})$ at $\vec{k} = 0$. When unit cell contains several atoms, the spin-wave energy is expressed e.g. in Ref. [19].

-
- [1] Hillebrands B, Hamrle J. Investigation of Spin Waves and Spin Dynamics by Optical Techniques. In: Handbook of Magnetism and Advanced Magnetic Materials Weinheim: Wiley-Interscience; 2007.
 - [2] Liu X, Steiner MM, Sooryakumar R, Prinz GA, Farrow RFC, Harp G 1996 *Phys. Rev. B* **53** 12166
 - [3] Buchmeier M, Kuanr BK, Gareev RR, Bürgler DE, Grünberg P 2003 *Phys. Rev. B* **67**(18) 184404
 - [4] Mock R, Hillebrands B, Sandercock R 1987 *J. Phys. E: Sci. Instrum.* **20** 656
 - [5] Hillebrands B 1999 *Rev. Scien. Instr.* **70** 1589
 - [6] Gaier O, Hamrle J, Hermsdoerfer SJ, Schultheiß H, Hillebrands B, Sakuraba Y, Oogane M, Ando Y 2008 *J. Appl. Phys.* **103**(10) 103910
 - [7] Demokritov SO, Hillebrands B, Slavin AN 2001 *Physics Reports* **348** 441
 - [8] Kalinikos BA, Slavin AN 1986 *J. Phys. C* **19** 7013
 - [9] Hillebrands B 1990 *Phys. Rev. B* **41** 530
 - [10] Rameev B, Yildiz F, Kazan S, Aktas B, Gupta A, Tagirov LR, Rata D, Buergler D, Grünberg P, Schneider CM, Kämmerer S, Reiss G, Hütten A 2006 *Phys. Stat. Sol. (a)* **203** 1503
 - [11] Kijima H, Ishikawa T, Marukame T, Koyama H, Matsuda K, Uemura T, Yamamoto M 2006 *IEEE Trans. Mag.* **42** 2688

- [12] Wang WH, Przybylski M, Kuch W, Chelaru LI, Wang J, Lu YF, Barthel J, Meyerheim HL, Kirschner J 2005 *Phys. Rev. B* **71**(14) 144416
- [13] Buchmeier M, Dassow H, Bürgler DE, Schneider CM 2007 *Phys. Rev. B* **75**(18) 184436
- [14] Hamrle J, Ferré J, Nývlt M, Višňovský v 2002 *Phys. Rev. B* **66**(22) 224423
- [15] Picozzi S, Continenza A, Freeman AJ 2006 *J. Phys. D: Appl. Phys.* **39**(5) 851
- [16] Ritchie L, Xiao G, Ji Y, Chen TY, Chien CL, Zhang M, Chen J, Liu Z, Wu G, Zhang XX 2003 *Phys. Rev. B* **68**(10) 104430
- [17] Stöhr J, Siegmann HC. Magnetism. From fundamentals to nanoscale dynamics. Springer; 2006
- [18] Pajda M, Kudrnovský J, Turek I, Drchal V, Bruno P 2001 *Phys. Rev. B* **64**(17) 174402
- [19] Kübler J, Fecher GH, Felser C 2007 *Phys. Rev. B* **76**(2) 024414
- [20] The dynamic magnetization is the difference between the static magnetization \vec{M}_0 and its actual instantaneous value $\vec{M}(t)$: $\vec{m}(t) = \vec{M}(t) - \vec{M}_0$.